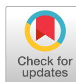

Recovery of an arenavirus entirely from RNA polymerase I/II-driven cDNA

Lukas Flatz[†‡], Andreas Bergthaler[†‡], Juan Carlos de la Torre[§], and Daniel D. Pinschewer[†¶]

[†]Institute of Experimental Immunology, Department of Pathology, University Hospital, Schmelzbergstrasse 12, 8091 Zurich, Switzerland; and [§]Molecular Integrative Neuroscience Department, The Scripps Research Institute, IMM-6, 10550 North Torrey Pines Road, La Jolla, CA 92037

Communicated by Rolf M. Zinkernagel, University Hospital of Zürich, Zürich, Switzerland, January 31, 2006 (received for review December 27, 2005)

The prototypic arenavirus lymphocytic choriomeningitis virus has been a primary workhorse of viral immunologists for almost a century, and it has served as an important model for studying basic principles of arenavirus molecular biology. Its negative-stranded bisegmented RNA genome has, however, posed a major obstacle to attempts at manipulating the infectious virus by reverse genetic techniques. Here, we report the recovery of infectious lymphocytic choriomeningitis virus (the immunosuppressive strain clone 13) entirely from cDNA. Intracellular transcription of the short and the long viral genome segment from polymerase (pol) I-driven vectors and coexpression of the minimal viral-transacting factors NP and L from pol II-driven plasmids resulted in the efficient formation of infectious virus with genetic tags in both genome segments. The cDNA-derived viruses behaved identically to wild-type virus in both cell culture and infected mice. Importantly, they caused a chronic infection and suppressed the adaptive immune response to an unrelated third-party virus. This technology provides an important basis for investigating viral determinants of persistent infection and immunosuppression. In addition, our findings demonstrate that pol I/II-based vector systems may represent an efficient alternative strategy for the recovery of cytoplasmic negative-strand RNA viruses from cDNA.

immunosuppression | lymphocytic choriomeningitis virus | reverse genetics | negative-strand RNA virus

The prototypic arenavirus lymphocytic choriomeningitis virus (LCMV) was first isolated in the 1930s (1, 2). Ever since, it has served as a primary workhorse in the fields of immunology and viral pathogenesis, contributing substantially to the development of multiple key concepts in both disciplines (reviewed in ref. 3). Among its many interesting aspects, LCMV has been particularly instrumental in the investigation of antiviral tolerance and virus-induced immunosuppression in persistent infection. Moreover, this virus may represent a neglected human pathogen (4). Over the years it has been found that, in addition to LCMV, a substantial number of other arenaviruses are widely distributed in the rodent populations of the entire world. Some of them, e.g., Lassa fever virus, a close relative of LCMV, and the New World viruses Junin, Machupo, and Guanarito, are of particular interest because they can cause hemorrhagic fevers with high lethality when accidentally transmitted to humans (5).

Arenavirus genomes consist of two single-stranded RNA segments, each of them encoding for two viral genes in ambisense orientation, separated by an intergenic region (IGR) that is predicted to fold into a secondary RNA structure of high stability. The short segment (S segment) expresses the viral surface glycoprotein (GP) and the nucleoprotein (NP) that encapsidates the viral genome and replicative intermediates (Fig. 1A). The long segment (L segment) carries the genes for the viral RNA-dependent RNA polymerase (pol) L and the small matrix protein Z. Despite their ambisense coding strategy, however, arenaviruses are negative-strand viruses, i.e., transfection of purified viral RNA into permissive cells does not initiate an infectious cycle, a fact that has long impeded the analysis of arenavirus molecular biology. Only relatively recently, a minireplicon system has been developed, allowing for the analysis of the viral cis-acting elements and transacting factors involved in transcription, replication, and particle formation (6–10), and similar systems have subsequently been described for Tacaribe virus and Lassa fever virus (11, 12). The LCMV reverse genetic system had initially been based on the intracellular expression of a viral model genome (MG) from T7 RNA pol (T7), combined with either T7-driven or pol II-driven coexpression of the minimal viral-transacting factors NP and L (6, 7). Owing to the virus's cytoplasmic life cycle, T7 had been the obvious choice for expression of an LCMV genome analogue. For orthomyxoviruses with a nuclear life cycle, however, pol I-driven vectors had long been accepted as a powerful method for expressing MGs and later for the efficient recovery of infectious viruses entirely from plasmid (reviewed in ref. 13). Stimulated by findings made in the bunyavirus field (14), we have also documented that pol I-driven vectors represented an efficient alternative means for expressing LCMV MG RNAs (9). Pol I-derived MG RNA species were exported to the cytoplasm where they assembled with plasmid-supplied L and NP proteins into ribonucleoproteins (RNPs) that were active in cytoplasmic transcription and replication (9). This system could even be exploited to reconstitute a recombinant full-length S-segment RNP. Upon reassortment with helper virus as a source for the L segment, an infectious LCM virus with an engineered S segment was recovered that expressed the GP of vesicular stomatitis virus (VSV) instead of the LCMV-GP (rLCMV/VSVG, ref. 15). In a reverse reassortment process, the VSVG-expressing S segment of this virus could be exchanged for a cDNA-derived S segment of interest, a strategy that was vastly facilitated by the potent selective capacity of VSV-neutralizing antibodies. Accordingly, viruses generated by this method have allowed us to study the role of the viral GP in liver disease (A.B., D. Merkler, E. Horvath, L. Bestmann, and D.D.P., unpublished work) and GP-based strategies to attenuate arenaviruses for use as live vaccines (A.B., N. U. Gerber, D. Merkler, E. Horvath, J.C.d.l.T., and D.D.P., unpublished work). Yet the arenavirus L segment harbors key determinants of the viral phenotype (16) that could not be studied in a reverse genetic manner. Here, we report that the intracellular expression of the LCMV RNA genome from pol I-driven vectors, combined with pol II-driven coexpression of the minimal transacting factors NP and L, resulted in the efficient recovery of infectious LCMV entirely from cDNA. This finding shows that pol I-driven systems may represent an efficient

Conflict of interest statement: No conflicts declared.

Abbreviations: LCMV, lymphocytic choriomeningitis virus; S segment, short segment; L segment, long segment; GP, glycoprotein; NP, nucleoprotein; MG, model genome; pol, polymerase; VSV, vesicular stomatitis virus; Cl13, clone 13; wtCl13, wild-type Cl13; ARM, Armstrong; IGR, intergenic region; L-IGR, L segment-IGR; RT, reverse transcription; PFU, plaque-forming units.

Data deposition: The sequences reported in this paper have been deposited in the GenBank database [accession nos. DQ361065 (S segment) and DQ361066 (L segment)].

[‡]L.F. and A.B. contributed equally to this work.

[¶]To whom correspondence should be addressed. E-mail: pinschi@pathol.unizh.ch.

© 2006 by The National Academy of Sciences of the USA

Downloaded from https://www.pnas.org by 18.97.9.175 on April 26, 2025 from IP address 18.97.9.175.

MICROBIOLOGY

Downloaded from https://www.pnas.org by 18.97.9.175 on April 26, 2025 from IP address 18.97.9.175.

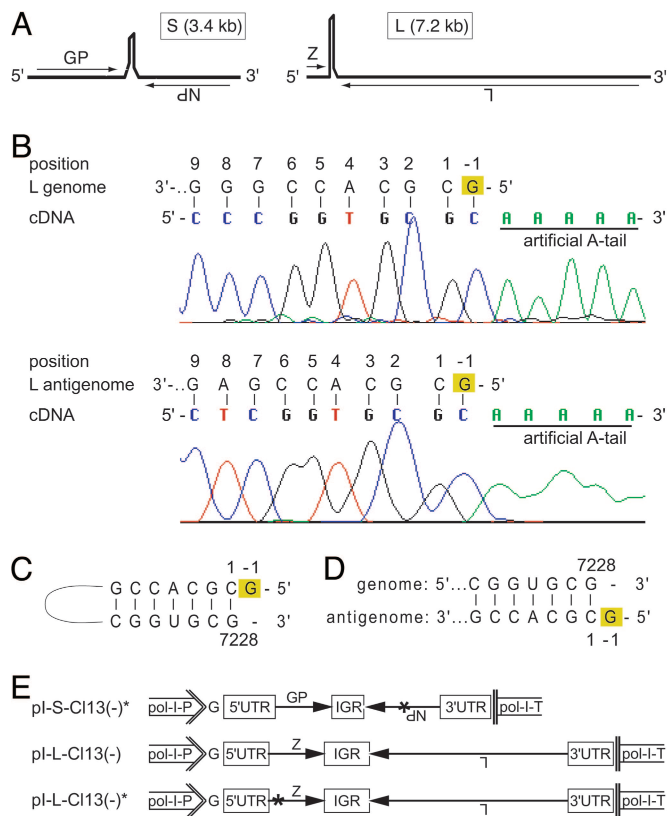

Fig. 1. Sequence of the LCMV L-IGR and 5′ terminus and genome expression vectors. (*A*) Schematic of the bisegmented LCMV genome with its four known genes (arrows). Inverted writing indicates antisense polarity. (*B*) Sequence analysis of the L-segment 5′ end was carried out as described in *Supporting Text*. The first-strand cDNA (cDNA) was A-tailed at its 3′ end for amplification by PCR and subsequent sequence analysis. The deducted 5′ terminal template sequence of the L-segment genome and antigenome, respectively, and their nucleotide positions are indicated (−1 to 9). Note the 5′ nontemplated G at position −1. (*C*) Intrasegment base-pairing and panhandle formation of the L-segment 5′ and 3′ terminal nucleotides with positions indicated. (*D*) Comparison of the L-segment antigenome 5′ end with its template, the L-segment genome 3′ terminus. Nucleotide positions are indicated. (*E*) Schematic description of the genome expression vectors used in this study. Noncoding genetic tags are indicated by *, cis-acting elements are boxed, and ORFs are labeled and represented as arrows. Inverted writing indicates antisense polarity. pol-I-P, pol I promoter; pol-I-T, pol I terminator.

alternative for the recovery of cytoplasmic negative-strand RNA viruses from cDNA. Moreover, the technology presented here and a simultaneously developed T7-driven system for the recovery of LCMV from cDNA (34) will provide powerful reverse genetic approaches for the study of the arenavirus immunobiology by using genetically engineered replication-competent viruses.

Results

We had observed that an LCMV L segment-based MG of ≈7.6 kb could be expressed from a pol I-driven vector and yielded reporter gene activity when the viral-transacting factors were coexpressed (D.D.P. and J.C.d.l.T., unpublished work). This finding lent support to the hypothesis that pol I should be able to express not only a full-length S segment (15) but also the L segment of LCMV (7.2 kb in length) for recognition by the viral-transacting factors. Thus, we set out to extend our previously published pol I/II-driven reverse genetic system for LCMV (9, 10, 15) to allow for the recovery of infectious virus entirely from plasmid. The previously published MG system and a partial rescue system for LCMV had been based on the Armstrong (ARM)53b strain (6, 9) that is unable to establish persistence in adult mice (17–19). With the intention of studying the virus–host relationship during chronic infection we therefore attempted to establish a complete rescue system for the ARM-derived variant clone 13 [Cl13 (17)] rather than for ARM itself. We first revisited the published Cl13 sequence [GenBank accession no. DQ361065 (S segment) and GenBank accession no. DQ361066 (L segment), compare with GenBank accession nos. M64450, J04331, and M27693, and ref. 20; for technical details see *Supporting Text*, which is published as supporting information on the PNAS web site] with an emphasis on the noncoding sequences of the L segment. The L-segment IGR (L-IGR) had previously been reported to exhibit substantial variability in length (21). Considering the important roles of the S-segment IGR in the viral life cycle (10), we reasoned that a correct L-IGR sequence was likely of importance for the efficient recovery of LCMV from plasmid. To overcome the intrinsic difficulties related to the predicted secondary RNA structures in the L-IGR, we used a heat-stable reverse transcription (RT) pol with helicase activity, followed by PCR amplification (for details see *Supporting Text*). Sequence analysis of the obtained PCR product readily yielded an L-IGR consensus sequence that was of the same length, although not of identical sequence, as the one recently published for LCMV-ARM53b (GenBank accession no. DQ361066, compare with GenBank accession nos. AY847351 and AY894816).

It had been demonstrated that arenavirus S segments carry a nontemplated G residue at their 5′ ends (22), but the precise 5′ terminus of the LCMV L segment was less certain (21, 23). For a Lassa fever virus S segment analogue it had, however, been shown that efficient template recognition by the viral RNA-dependent RNA pol depended critically on the precise 5′ end (12), and we have made similar observations for the LCMV S segment (ref. 8 and D.D.P and J.C.d.l.T. unpublished work). Thus, we analyzed the Cl13 L segment 5′ ends by using a 5′ RACE protocol that was based on A-tailing of first-strand cDNA with terminal deoxynucleotidyl transferase (for technical details see *Supporting Text*). This approach unambiguously revealed a G residue at position −1 on both the LCMV L-segment genome and antigenome (Fig. 1*B*). Different investigators (24–26) have unequivocally shown that the 3′ end of the L-segment genome terminates on a G residue and not on a C (Fig. 1 *C* and *D*). Thus, intramolecular annealing of the genome into a panhandle structure [the putative viral promoter (8), Fig. 1*C*] does not form a flush end as for most negative-strand RNA viruses (22). Also, this finding suggests that the 5′ G of antigenomes found here represents a nontemplated base like in the S segment (ref. 22 and Fig. 1*D*). An analogous conclusion for the L-segment genome 5′ G, although likely, however, awaits formal determination of its template, i.e., of the antigenome 3′ end.

Based on this sequence information we assembled Cl13 S- and L-segment cDNAs containing the master consensus sequence and cloned them in genomic polarity under control of the mouse pol I promoter and terminator cassettes (14). Thereby we obtained the plasmids pI-S-Cl13(−)* and pI-L-Cl13(−), respectively (Fig. 1*E*). pI-S-Cl13(−)* was partially based on a previously published backbone [pS-Bsm(−) (15)] that contained a noncoding single-nucleotide tag, deleting an EcoNI site for discrimination from wild-type virus (Fig. 2*C*). In contrast, pI-L-Cl13(−) was assembled *de novo* and did not contain a genetic tag. A second constructs was also generated [pI-L-Cl13(−)*, Fig. 1*E*] that differed from the wild-type Cl13 (wtCl13) sequence by a noncoding single-nucleotide transition in the Z ORF. Thereby an additional AvaII recognition site was introduced (Fig. 2*C*). The NP ORFs of ARM53b and Cl13 are identical, and hence the available pol II-driven expression plasmid pC-NP (7) could also be used here for intracellular coexpression of this viral protein. The previously published plasmid for intracellular ex-

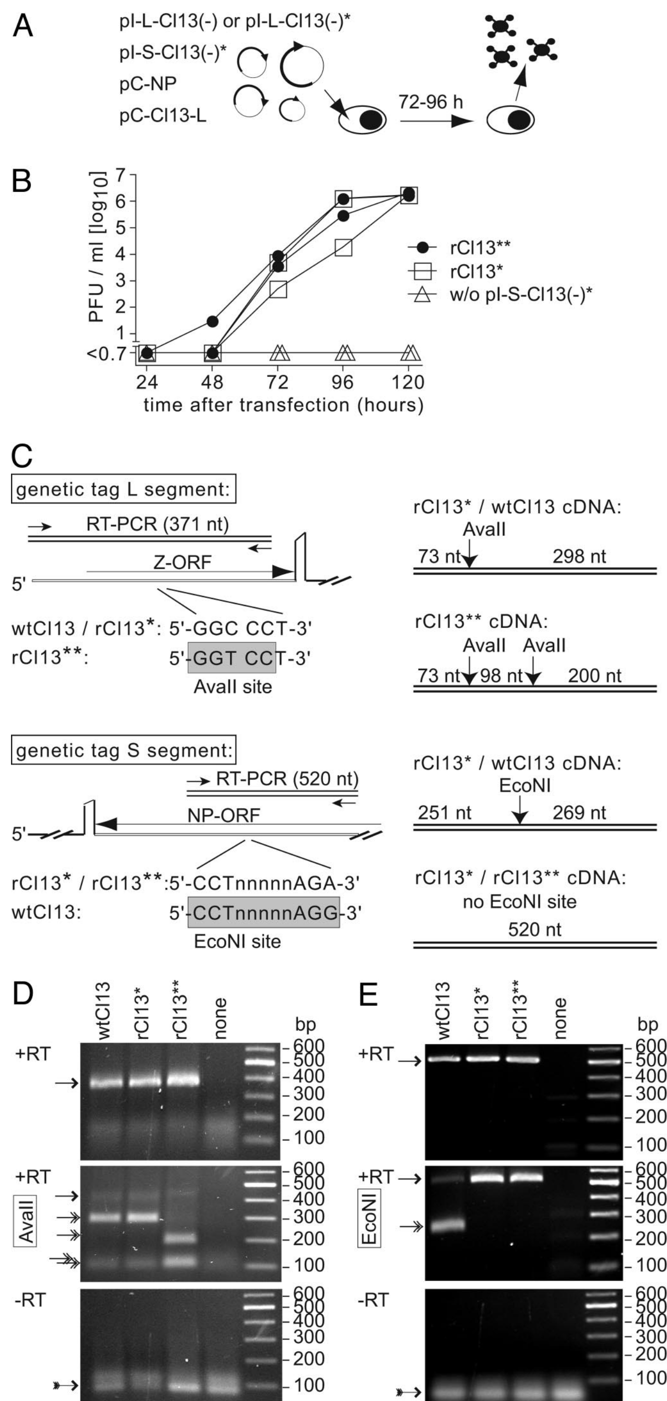

Fig. 2. Recovery of genetically tagged Cl13 entirely from cDNA. (*A* and *B*) As outlined schematically in *A*, subconfluent BHK-21 cells in M6 tissue culture wells were transfected with 0.8 μg of pC-NP, 1 μg of pC-Cl13-L, 0.8 μg of pI-S-Cl13(−)*, and either 1.4 μg of pI-L-Cl13(−) to recover rCl13* or 1.4 μg of pI-L-Cl13(−)* to recover rCl13**. In negative control wells [without (w/o) pI-S-Cl13(−)*], the pI-S-Cl13(−)* plasmid was substituted for an MG expression plasmid lacking LCMV structural genes and expressing GFP instead (9). (*B*) Culture supernatant was collected at the indicated time points and tested for viral infectivity by immunofocus assays. Symbols represent individual culture wells. (*C*) Schematic description of the genetic tags in the S- and L-segment cDNAs. The stretches of viral RNA amplified by RT-PCR and the predicted fragments obtained from restriction digestion are indicated. (*D* and *E*) Fresh BHK-21 cells were infected with wtCl13, rCl13*, and rCl13** at multiplicity of infection of 0.1 or left uninfected (none). Forty-eight hours later, total cellular RNA was harvested and processed for RT-PCR amplification. L segment-specific (*D*) and S segment-specific (*E*) amplification products (+RT, *Top*) yielded the expected fragments upon digestion with AvaII or EcoNI, respectively (*Middle*), and were fully RT-dependent (compare with −RT, *Bottom*). Single-headed arrow: undigested PCR product; double-headed arrow: digested fragments; feathered arrow: primer dimers.

pression of the ARM53b L ORF under control of pol II [pC-L (7)] differed, however, from our Cl13 sequence at four coding positions, and hence a plasmid was generated (pC-Cl13-L) expressing the Cl13 L ORF (master consensus sequence) under control of the same pol II expression cassette (27).

As schematically depicted in Fig. 2*A*, cotransfection of BHK-21 cells with pC-NP, pC-Cl13-L, pI-S-Cl13(−)*, and either pI-L-Cl13(−) or pI-L-Cl13(−)* resulted within ≈72–96 h in the recovery of high titers of infectious virus from the culture supernatant (Fig. 2*B*). Notably, this result was obtained at the first try by using standard lipofection procedures. Moreover, the recovery was highly reproducible i.e., from a total of >30 individual M6 tissue culture wells that were transfected in multiple experiments all but one yielded infectious virus, underscoring the high efficiency of the system. To ascertain the viral origin from cDNA we tested for the presence of the genetic tags in the viral genome. The virus obtained when transfecting pI-S-Cl13(−)* and pI-L-Cl13(−) will be referred to as rCl13*, whereas the virus derived from pI-S-Cl13(−)* and pI-L-Cl13(−)* was named rCl13** to indicate the expected genetic tags in only one or both genome segments, respectively. Fresh BHK-21 cells were infected with rCl13*, rCL13**, or wtCl13 for comparison, and RT-PCRs were carried out to amplify viral RNA stretches spanning the expected genetic tags in the S and L segments (schematically depicted in Fig. 2*C*). All PCR products were RT-dependent, excluding residual plasmid contamination in the virus preparations that might have confounded the subsequent analysis (Fig. 2*D*). As expected, the S segment-derived amplification product of wtCl13 was sensitive to digestion with EcoNI, whereas the products derived from rCl13* and rCl13** were not. The L segment-derived RT-PCR products of wtCl13 and rCl13* yielded identical fragments when digested with AvaII, whereas rCl13** yielded smaller ones as predicted (Fig. 2*C*). Hence, rCl13* and rCl13** were derived from the transfected parental plasmids.

Next, we compared the growth curves of rCl13* and rCl13** with wtCl13 in cell culture and found them to be indistinguishable (Fig. 3*A*). To also compare viral replication kinetics *in vivo*, C57BL/6 mice were infected i.v. with 2×10^6 plaque-forming units (PFU) of wtCl13, rCl13*, rCl13**, or ARM53b as a control virus that is unable to persist in adult mice. Upon infection with wtCl13, rCl13*, or rCl13**, high-titer viremia was established within 4 days, lasting for at least 29 days. In contrast, ARM53b was cleared from the blood within 8 days after infection. We also verified that the viral populations persisting in rCl13*- and rCl13**-infected mice still carried the genetic tags. Viral RNA was extracted from the serum of mice at day 12 after infection, and RT-PCR products were tested by restriction digestion as outlined above. The analysis yielded the same result as shown in Fig. 2*D* for tissue culture infections, confirming that the genetic tags were stably expressed (Fig. 5, which is published as supporting information on the PNAS web site).

Persistent infection with Cl13 is known to subvert both the LCMV-specific CTL response to immunodominant epitopes and the adaptive immune response to unrelated third-party infections (18, 28). To test whether the cDNA-derived viruses shared the ability of wtCl13 to cause such an acquired immunodeficiency syndrome, the above groups of mice and uninfected controls were challenged with 2×10^6 PFU of VSV i.p. on day 22 after primary infection (Fig. 4). Serum was collected on days 25 and 29 (i.e., days 3 and 7 after VSV challenge, respectively) to determine VSV-neutralizing antibody titers. ARM-infected mice mounted virtually unimpaired IgM responses on day 25, followed by isotype class switch and neutralizing IgG titers on

Downloaded from https://www.pnas.org by 18.97.9.175 on April 26, 2025 from IP address 18.97.9.175.

PNAS PNAS PNAS PNAS

Downloaded from https://www.pnas.org by 18.97.9.175 on April 26, 2025 from IP address 18.97.9.175.

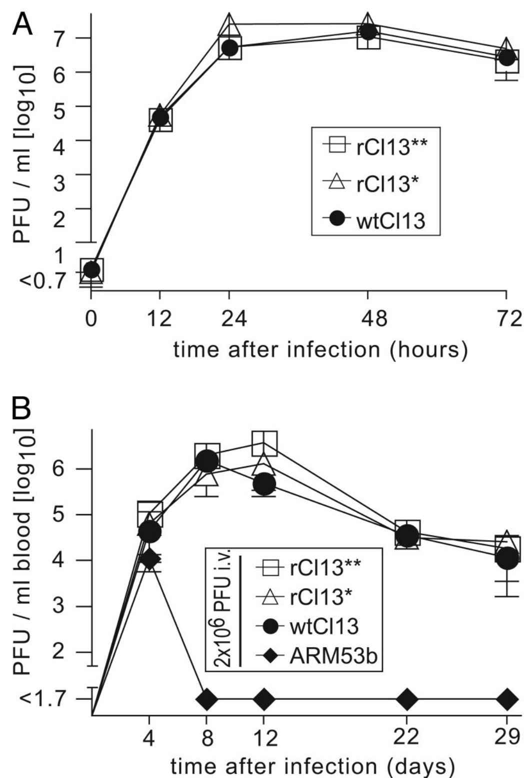

Fig. 3. Propagation of cDNA-derived viruses in cell culture and infected mice. (*A*) Subconfluent BHK-21 cells in M6 tissue culture wells were infected with wtCl13, rCl13*, or rCl13** at multiplicity of infection of 0.01. Supernatant was collected at the indicated time points for determination of viral titers. Symbols represent the mean ± SD of three individual culture wells. (*B*) C57BL/6 mice were infected with 2×10^6 PFU of ARM53b, wtCl13, rCl13*, or rCl13**. Blood was collected at the indicated time points for the assessment of viral titers. Symbols represent the mean ± SD of four mice per group. One representative experiment of two is shown.

day 29 that were in a similar range as in mice that had not undergone prior infection with LCMV (Fig. 4*A*). In marked contrast, these responses were suppressed to below detection levels in mice that were persistently infected with wtCl13, rCl13*, or rCl13**. The early IgM response (i.e., day 3 after VSV infection) is known to be T cell-independent, whereas isotype class switch and the production of IgG is $CD4^+$ T cell-dependent, indicating that the cDNA-derived viruses rCl13* and rCl13** shared the ability of wtCl13 to suppress both of these immune functions. Moreover, persistent infection with one of these three viruses caused a marked suppression of the VSV-specific $CD8^+$ T cell response, whereas ARM infection did not (Fig. 4*B*). As expected, persistent infection with wtCl13, rCl13*, or rCl13** also resulted in the exhaustion of the $CD8^+$ T cell response to the immunodominant LCMV epitope NP396, whereas NP396-specific IFN-γ-producing $CD8^+$ T cells were readily detected in ARM-infected mice (Fig. 4*B*). Taken together, the *in vivo* behavior of the cDNA-derived and genetically tagged rCl13* and rCl13** viruses was indistinguishable from wtCl13, validating our pol I-based reverse genetic system for the analysis of the virus–host relationship in adult persistent LCMV infection. Importantly, two viruses recovered from different L-segment expression plasmids (rCl13* and rCl13**) exhibited an identical phenotype. This is an additional indication for the high reproducibility of our reverse genetic system, a property that will be of paramount importance for future studies addressing the impact of individual point mutations on viral immunobiology.

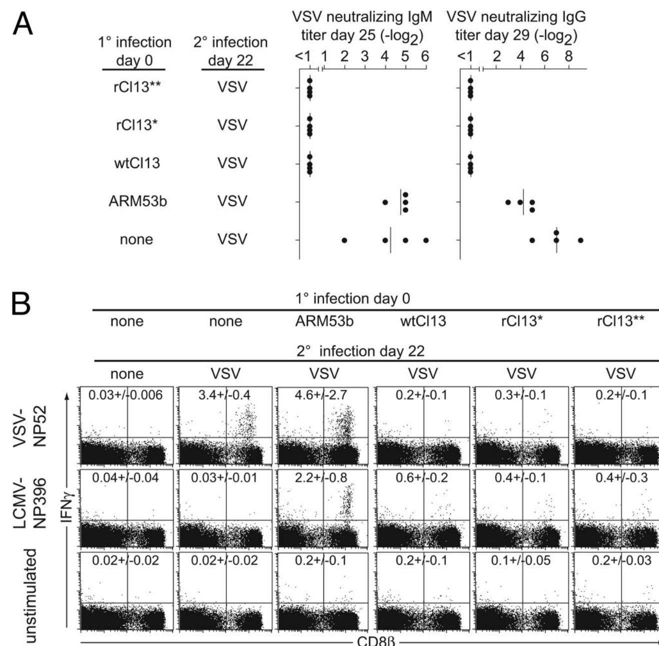

Fig. 4. Suppression of B cell and T cell responses by the cDNA-derived viruses. On day 0, C57BL/6 mice (same mice as in Fig. 3*B*) were infected i.v. (1° infection) with 2×10^6 PFU of ARM53b, wtCl13, rCl13*, or rCl13**, or they were left uninfected (none). Twenty-two days later, the indicated groups of mice were challenged with 2×10^6 PFU of VSV i.p. (2° infection). (*A*) On days 25 and 29 (3 and 7 days after secondary infection), serum samples were collected for determination of VSV-neutralizing IgM (day 25) and neutralizing IgG (day 29). Symbols represent individual mice. One representative experiment of two is shown. (*B*) On day 30, the mice were killed, and the frequency of splenic IFN-γ-producing $CD8^+$ T cells specific for either the immunodominant VSV NP-derived epitope NP52 or the LCMV NP-derived epitope NP396 was determined in an intracellular cytokine assay. Background IFN-γ production is shown for comparison (unstimulated). The frequency of IFN-γ-producing $CD8^+$ cells within the total $CD8^+$ T cell compartment is indicated for each representative FACS plot. Numbers indicate the mean ± SD of three mice per group.

Discussion

Unlike for all of the other known families of negative-strand RNA viruses (13, 29), arenaviruses have to our knowledge not previously been recovered entirely from cloned cDNA, and the same seems to be the case for bona fide ambisense viruses. With this study and a simultaneous study by Sanchez and de la Torre (34), these hurdles have been overcome. Here, we have exploited pol I-driven vectors for expression of the viral genome segments, a strategy that is against current practice for a cytoplasmic virus like LCMV. A T7-based rescue system, as exploited by A. B. Sanchez and J.C.d.l.T. (34), would have represented the obvious method of choice. It has been known for a while, however, that viruses with a nuclear life cycle such as influenza A can be recovered by using either T7- or pol I-driven systems (13). As shown here, the same holds true for cytoplasmic viruses. This possibility had previously been suggested by pol I-based MG systems for bunyaviruses, filoviruses, and arenaviruses (9, 14, 30), but a complete pol I-based rescue of an infectious negative-strand virus with a cytoplasmic life cycle has to our knowledge not previously been reported. The rescue system of choice for a particular virus may therefore not depend only on its intracellular compartment of replication. The differential proneness of T7 or pol I to terminate prematurely at terminator-like sequences within a given viral genome may represent only one of many factors that may be difficult to predict but could substantially influence the efficiency of virus recovery. In addition, pol I-based systems render the use of a 3′ terminal ribozyme unnecessary

because, unlike for T7, transcription termination at the pol I terminator is of high precision. Ribozymes, however, can be of limited cleavage efficiency requiring modifications on the transcript 3′ terminus (8). In favor of T7-driven systems speaks their functionality in virtually any cell type, whereas pol I expression cassettes are relatively species-specific, e.g., the vector used here operates almost exclusively in rodent cells. Furthermore, the use of a pol I/II-driven system bears the potential risk for unintentional splicing of the primary transcripts, which may prevent the successful application of our rescue strategy to specific arenaviruses or strains.

We have expressed viral RNA segments of genomic (−) polarity bearing the potential risk of hybrid arrest, i.e., the annealing of L- and NP-mRNAs with the unencapsidated genomic L- and S-segment RNAs, respectively. It had been proposed that this process could prevent ribonucleoprotein formation and thereby the initiation of the infectious cycle. The efficient recovery of virus by using genomic polarity transcripts does not exclude that hybrids form, but it suggests that hybrid arrest was not a major limiting factor in this setting. Preliminary data suggest, however, that virus can also be recovered when RNA of antigenomic polarity is expressed (data not shown). For future attempts at rescuing other arenaviruses from cDNA, it may be worth trying both polarities in parallel to enhance the likelihood that other potential pitfalls like terminator-like sequences in the transcript (see above) can be avoided.

The LCMV rescue system for Cl13 presented here and the T7-driven LCMV rescue system (34) should enable us to tackle a number of long-standing questions about the virus's molecular biology, its relationship with the host cell, and the specific role of the four known viral genes in various models of viral pathogenesis (3, 16, 18, 19). Chronic infection with Cl13 represents one of the prototypical small-animal models for investigating basic mechanisms of T cell dysfunction in chronic infection and viral interference with antigen presentation as a substrate of virus-induced immunosuppression (18, 19). The ability for directed engineering of the entire LCMV genome will offer unique opportunities for investigating the viral determinants thereof and studying the immunological pressure exerted on the persisting virus. In addition, the methodology and vector combinations used here should allow for the rescue of other arenaviruses, including Lassa fever virus and the South American hemorrhagic fever viruses, from plasmid. This technology may accelerate the development and fine-tuning of live-attenuated arenavirus vaccines (16) and may substantially facilitate their safe production for use in endemic areas where they are urgently needed (5, 31).

Materials and Methods

Plasmids, Cells, and Transfections. The pC-NP plasmid has been described (7, 8). For generation of pC-L-Cl13, the Cl13 L ORF was amplified by RT-PCR in three separate fragments that were merged for insertion into the pC backbone (27), analogously to a strategy described for Lassa fever virus (ref. 12 and see Fig. 6, which is published as supporting information on the PNAS web site). pI-S-Cl13(−)* was generated by inserting a Cl13-GP cDNA into the pS-Bsm(−) backbone that expresses under the control of pol I a LCMV S-segment cDNA with a linker instead of the GP ORF (15). pI-L-Cl13(−) is based on the same pol I vector as pI-S-Cl13(−)* (14) and was assembled in a multistep cloning procedure from RT-PCR fragments with master consensus sequence (for details of the cloning strategy see Fig. 6; primers used for cloning of the L-segment constructs are listed in Table 1, which is published as supporting information on the PNAS web site). The AvaII site in the Z ORF was introduced in a standard two-way PCR approach. Additional primer sequences and PCR conditions are available on request. BHK-21 cells were transfected by using Lipofectamin (3 μl/μg DNA; Invitrogen).

Viruses, Viral Immunofocus Assay, and Identification of Genetic Tags. The ARM-derived variant Cl13 (17) was obtained from Rafi Ahmed (Emory Vaccine Center, Atlanta), and passage 5 was used for RT-PCR cloning and mouse experiments. ARM53b was obtained from Michael Buchmeier (The Scripps Research Institute). LCMV titers were determined in a NP-specific immunofocus assay as described (32).

For identification of the genetic tags, total cellular RNA was extracted from virus-infected cells by using Trizol (Invitrogen) or from mouse serum by using the QIAamp viral RNA mini kit (Qiagen, Valencia, CA). RT was carried out with random hexamers by using Superscript II RT pol (Invitrogen), and *Taq* pol (NEB, Beverly, MA) was used for PCR with gene-specific primers 5′-GCATTGTCTGGCTGTAGCTTA-3′ and 5′-CAATGACGTTGTACAAGCGC-3′ for the S segment or with primers 5′-*TATGAAGACAGAGGT*GCGCACCGGGGATCCTAGGCGTTTAG-3′ (unpaired overhang in italics) and 5′-CTTCGTAGGGAGGTGGAGAG-3′ for the L segment. EcoNI or AvaII digestion of the PCR products was performed without prior purification, which explained occasionally incomplete digestion.

Mice and Animal Experiments. C57BL/6 mice were bred at the Institut für Labortierkunde at the University of Zurich and housed under specific pathogen-free conditions for the experiments. All animal studies were carried out with authorization by the Kantonale Veterinäramt and in accordance with Swiss law for animal protection.

Intracellular Cytokine Assay and VSV Neutralization Assays. Peptide stimulation and intracellular staining for IFN-γ have been described (33). Anti-CD8α-phycoerythrin and anti-IFN-γ-allophycocyanin were purchased from Pharmingen. VSV neutralization assays were carried out as described (32). Neutralizing IgG was measured by 2-mercaptoethanol resistance because secondary antibodies could not be used (32). Neutralizing activity exceeding the 2-mercaptoethanol-resistant fraction by 4-fold or more was considered IgM.

Viral Sequence Analysis. Sequencing protocols are outlined in detail in *Supporting Text*. Briefly, Cl13 virion RNA was purified, and cDNA was generated with gene-specific primers by using superscript II RT pol (Invitrogen) or Omniscript RT pol (Qiagen) for the L-IGR. PCR was carried out with PFU Turbo (Stratagene) or Amplitaq Gold (PerkinElmer) for the L-IGR. PCR products were either sequenced directly or first cloned into the pGEMT vector (Promega). The S-segment terminal sequences were determined by a RNA circularization-based protocol. For 5′ RACE analysis of the L-segment termini, protocols were adapted from the Invitrogen kit manual, *3′RACE System for Rapid Amplification of cDNA Ends*.

We thank Urs Schneider, Rima Youil, and Mar Perez for helpful discussions; Edit Horvath for excellent technical assistance; and Dieter Zimmermann for sequencing services. A.B. holds a Ph.D. fellowship from the Boehringer Ingelheim Fonds. This work was supported by Swiss National Science Foundation Grant 3100A0-104067/1 (to D.D.P.).

1. Armstrong, C. & Lillie, R. D. (1934) *Public Health Rep.* **49,** 1019–1027.
2. Rivers, T. M. & Scott, T. F. M. (1935) *Science* **81,** 439–440.
3. Zinkernagel, R. M. (2002) *Curr. Top. Microbiol. Immunol.* **263,** 1–5.
4. Wright, R., Johnson, D., Neumann, M., Ksiazek, T. G., Rollin, P., Keech, R. V., Bonthius, D. J., Hitchon, P., Grose, C. F., Bell, W. E. & Bale, J. F., Jr. (1997) *Pediatrics* **100,** E9.
5. Geisbert, T. W. & Jahrling, P. B. (2004) *Nat. Med.* **10,** S110–S121.
6. Lee, K. J., Novella, I. S., Teng, M. N., Oldstone, M. B. & de la Torre, J. C. (2000) *J. Virol.* **74,** 3470–3477.
7. Lee, K. J., Perez, M., Pinschewer, D. D. & de la Torre, J. C. (2002) *J. Virol.* **76,** 6393–6397.
8. Perez, M. & de la Torre, J. C. (2003) *J. Virol.* **77,** 1184–1194.
9. Pinschewer, D. D., Perez, M. & de la Torre, J. C. (2003) *J. Virol.* **77,** 3882–3887.
10. Pinschewer, D. D., Perez, M. & de la Torre, J. C. (2005) *J. Virol.* **79,** 4519–4526.

Downloaded from https://www.pnas.org by 18.97.9.175 on April 26, 2025 from IP address 18.97.9.175.

11. Lopez, N., Jacamo, R. & Franze-Fernandez, M. T. (2001) *J. Virol.* **75,** 12241–12251.
12. Hass, M., Golnitz, U., Muller, S., Becker-Miaja, B. & Gunther, S. (2004) *J. Virol.* **78,** 13793–13803.
13. Neumann, G., Whitt, M. A. & Kawaoka, Y. (2002) *J. Gen. Virol.* **83,** 2635–2662.
14. Flick, R. & Pettersson, R. F. (2001) *J. Virol.* **75,** 1643–1655.
15. Pinschewer, D. D., Perez, M., Sanchez, A. B. & de la Torre, J. C. (2003) *Proc. Natl. Acad. Sci. USA* **100,** 7895–7900.
16. Lukashevich, I. S., Patterson, J., Carrion, R., Moshkoff, D., Ticer, A., Zapata, J., Brasky, K., Geiger, R., Hubbard, G. B., Bryant, J. & Salvato, M. S. (2005) *J. Virol.* **79,** 3934–3942.
17. Ahmed, R., Salmi, A., Butler, L. D., Chiller, J. M. & Oldstone, M. B. (1984) *J. Exp. Med.* **160,** 521–540.
18. Sevilla, N., Kunz, S., Holz, A., Lewicki, H., Homann, D., Yamada, H., Campbell, K. P., de la Torre, J. C. & Oldstone, M. B. (2000) *J. Exp. Med.* **192,** 1249–1260.
19. Barber, D. L., Wherry, E. J., Masopust, D., Zhu, B., Allison, J. P., Sharpe, A. H., Freeman, G. J. & Ahmed, R. (2005) *Nature* **439,** 682–687.
20. Salvato, M., Borrow, P., Shimomaye, E. & Oldstone, M. B. (1991) *J. Virol.* **65,** 1863–1869.
21. Salvato, M. S. & Shimomaye, E. M. (1989) *Virology* **173,** 1–10.
22. Garcin, D. & Kolakofsky, D. (1990) *J. Virol.* **64,** 6196–6203.
23. Meyer, B. J. & Southern, P. J. (1994) *J. Virol.* **68,** 7659–7664.
24. Romanowski, V. & Bishop, D. H. (1985) *Virus Res.* **2,** 35–51.
25. Auperin, D. D., Compans, R. W. & Bishop, D. H. (1982) *Virology* **121,** 200–203.
26. Salvato, M., Shimomaye, E. & Oldstone, M. B. (1989) *Virology* **169,** 377–384.
27. Niwa, H., Yamamura, K. & Miyazaki, J. (1991) *Gene* **108,** 193–199.
28. Leist, T. P., Ruedi, E. & Zinkernagel, R. M. (1988) *J. Exp. Med.* **167,** 1749–1754.
29. Schneider, U., Schwemmle, M. & Staeheli, P. (2005) *Proc. Natl. Acad. Sci. USA* **102,** 3441–3445.
30. Groseth, A., Feldmann, H., Theriault, S., Mehmetoglu, G. & Flick, R. (2005) *J. Virol.* **79,** 4425–4433.
31. McCormick, J. B., Webb, P. A., Krebs, J. W., Johnson, K. M. & Smith, E. S. (1987) *J. Infect. Dis.* **155,** 437–444.
32. Pinschewer, D. D., Perez, M., Jeetendra, E., Bächi, T., Horvath, E., Hengartner, H., Whitt, M. A., de la Torre, J. C. & Zinkernagel, R. M. (2004) *J. Clin. Invest.* **114,** 988–993.
33. Probst, H. C., Tschannen, K., Gallimore, A., Martinic, M., Basler, M., Dumrese, T., Jones, E. & van den Broek, M. F. (2003) *J. Immunol.* **171,** 5415–5422.
34. Sanchez, A. B. & de la Torre, J. C. (2006) *Virology*, in press.

Downloaded from https://www.pnas.org by 18.97.9.175 on April 26, 2025 from IP address 18.97.9.175.